Available online at www.sciencedirect.com
SCIENCE DIRECT
ELSEVIER
International Journal of Mass Spectrometry 252 (2006) 151–156
International Journal of Mass Spectrometry
www.elsevier.com/locate/ijms

First observation of delayed electron emission from dianionic metal clusters

Alexander Herlert *, Lutz Schweikhard

Institut für Physik, Ernst-Moritz-Arndt-Universität, 17487 Greifswald, Germany

Received 11 November 2005; received in revised form 10 January 2006; accepted 11 January 2006
Available online 14 March 2006

Abstract

Time-resolved electron emission after photoexcitation in a Penning trap has been applied to size and charge-state selected dianionic gold clusters, Au_{29}^{2-}. An exponential decrease of the relative abundance was recorded, along with a corresponding appearance of the monoanion Au_{29}^{1-}. This constitutes the first observation of delayed electron emission from a metal-cluster dianion. By application of the Weisskopf decay-rate model to the emission rate the binding energy of the second surplus electron was found to be 0.91(5) eV. This value compares favourably with the second electron affinity as expected from the liquid drop model.

Keywords: Penning trap; Metal clusters; Photoexcitation; Dianions

1. Introduction

When atomic clusters are excited they can respond by several decay channels. The corresponding branching ratios depend on the element, cluster size, and charge state under consideration. For the mostly studied positively charged clusters the energy for further ionization is usually larger than the atomic binding energy. Thus, electron emission is suppressed with respect to, e.g., monomer evaporation. However, in the case of negatively charged clusters the binding energy becomes comparable and the electron-emission channel opens up [1,2]. With the recent availability of multiply negatively charged metal clusters [3,4] the investigation of binding energies and decay pathways can now be extended to various new charge states.

Gas-phase dianions have found an increased interest in the last years, where numerous studies have been reported for molecules and clusters (see [5] and references therein). The Coulomb barrier plays an important role and is a stabilizing element of the multianions [6]. In any case it influences the decay behavior. For example, tunneling of the surplus electrons through the barrier was observed for molecular dianions [7,8] and fullerene dianions [9].

At the ClusterTrap experiment the production of doubly and triply charged metal-cluster anions has been studied in detail [10]. Already for the production in the trap the relative abundance of the dianionic metal clusters showed a characteristic pattern: larger yields for cluster sizes that reach a closed electronic shell by the attachment of a further electron to the monoanion and a decreased dianion yield in those cases where the monoanions already have a filled electronic shell [10–12].

First preliminary experiments on the photoexcitation and collisional activation showed both electron emission and monomer evaporation from gold-cluster dianions [13,14]. For cationic clusters time-resolved measurements [15] have been performed extensively in order to determine dissociation energies [16,17].

In the present work, these approaches have been combined and the method of monitoring the delayed decay after pulsed photoexcitation in a Penning trap is demonstrated for gold-cluster dianions. For the first time the delayed electron emission from a doubly negative charged metal cluster has been observed.

2. Experimental setup and procedure

The ClusterTrap experiment consists of a laser-vaporization source, a Penning trap for ion storage and interaction, and a time-of-flight (TOF) mass spectrometer for the analysis of the

* Corresponding author. Present address: CERN, Physics Department, 1211 Geneva 23, Switzerland.
E-mail address: alexander.herlert@cern.ch (A. Herlert).

1387-3806/$ – see front matter © 2006 Elsevier B.V. All rights reserved.
doi:10.1016/j.ijms.2006.01.051

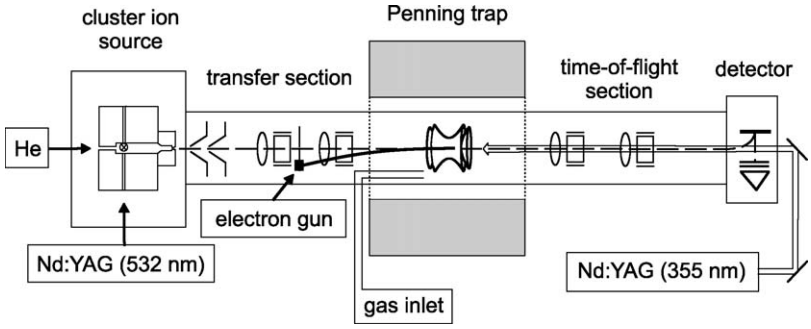

Fig. 1. Sketch of the experimental setup.

ion ensemble after various reactions [18]. A sketch of the experimental setup is shown in Fig. 1.

For the production of dianionic metal clusters, singly charged cluster anions from the ion source are transferred to the Penning trap. After size selection they are subjected to a bath of simultaneously stored electrons. These low-energy electrons are created by guiding an electron beam from an external electron gun through the center of the ion trap, which ionizes argon-gas atoms that are pulsed into the trap volume [3,10].

The singly charged cluster anions that do not catch a further electron from the electron cloud are removed from the trap with the same procedure as applied for the inital size selection: the cyclotron radius of the ion motion is increased with a resonant dipolar radio frequency excitation until the ions leave the trap radially. Since before the electron attachment the clusters are already size selected and since there is no decay observed during electron attachment, the resulting cluster ensemble is both size and charge-state selected. As an example, a typical TOF spectrum before photoexcitation of Au_{29}^{2-} is shown in Fig. 2(a). In addition, the dianionic clusters are centered in the middle of the trap by a buffer-gas cooling technique [19]. In this process an equilibration to room-temperature energies is achieved, too. Next, to avoid any interaction of the simultaneously stored low-energy electrons in the forthcoming excitation steps, the potential of the endcap electrodes is lowered for a duration of 1 μs, which allows the fastly moving electrons to leave the trap axially whereas the slowly moving cluster dianions stay stored ("suspended trapping" [20]).

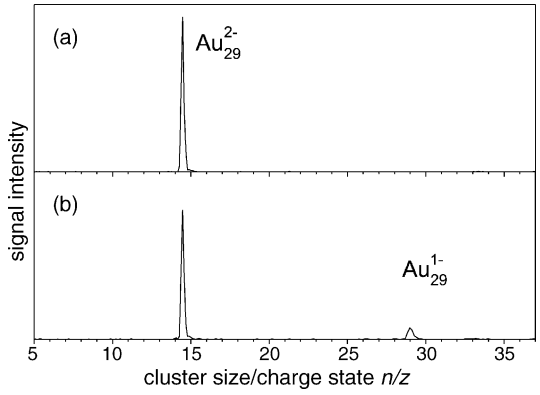

Fig. 2. TOF spectrum before (a) and after photoexcitation (b) of size and charge-state selected Au_{29}^{2-}.

After these preparations the dianions are excited with a 10-ns pulse of the third harmonic (λ = 355 nm) of a Nd:YAG laser. The pulse energy is 1 mJ with a FWHM of the Gaussian beam profile of about 8 mm. Note that the cluster ion cloud has a width of about 1 mm after the buffer-gas centering [21], thus all stored ions see the laser beam with almost the same fluence.

In order to monitor the decay process time-resolved, the duration after the excitation until the ejection into the TOF mass spectrometer is varied from 10 μs up to 100 ms. Thus, the procedure is analogue to a recent pilot experiment on singly charged metal-cluster anions [22]. As an example, a TOF spectrum after photoexcitation of Au_{29}^{2-} and a delay time of 100 ms is shown in Fig. 2(b).

3. Results

The different decay pathways have each a characteristic pattern in the recorded mass spectra. The evaporation of a neutral monomer leads to the appearance of the next smaller cluster size in the TOF spectrum, i.e., the product system is observed like the precursor cluster (4π detection efficiency). In contrast, the emission of an electron from a singly charged anion leads to the loss of clusters from the trap. For dianions the product cluster is still charged after the emission of an electron and is thus observed in the TOF spectrum.

In Fig. 3, the relative abundances of Au_{29}^{2-} and the product Au_{29}^{1-} are plotted as a function of the delay between photoexcitation and TOF mass analysis. Note that the abundances have been normalized to the sum of cluster signals within a given spectrum and to the result of alternated cycles with a fixed delay of 100 ms; for details see [22]. This procedure corrects for the shot-to-shot variations of the cluster source and to variations of the laser irradiation, respectively. However, the information on a possible loss of precursor ions by emission of two electrons is lost. In a separate experiment such a loss of about 10–20% has been observed. It was independent of the delay, i.e., the corresponding decay was faster than the present time window (<10 μs).

As in the previous investigation on singly charged gold-cluster anions [22] an oscillation of the ion yield is observed which is superposed on an exponential behavior. A fit of the

Table 1
Fit parameters after application of Eq. (1) to the relative abundance of Au_{29}^{2-} and Au_{29}^{1-} as shown in Fig. 3

	c_1	c_2	c_3	$\tau = k^{-1}$ (ms)	γ (s^{-1})	$\omega(2\pi)^{-1}$ (Hz)	ϕ (°)
Au_{29}^{2-}	1	0.022(4)	0.034(6)	4.3(2.0)	187(89)	1305(14)	76(10)
Au_{29}^{1-}	1	−0.23(4)	0.35(6)	7.6(5.7)	121(92)	1305(13)	76(9) + 180

The parameter c_1 has been fixed to 1 which is the expected value for $t \to \infty$.

function

$$r(t) = c_1 + c_2\, e^{-kt} + c_3\, e^{-\gamma t} \sin(\omega t + \phi) \quad (1)$$

has been performed with the (angular) oscillation frequency ω, the damping constant γ of the oscillation, and the phase ϕ of the oscillation at $t = 0$.

The oscillation frequency is found to be $\omega/2\pi = 1305(14)$ and 1305(13) Hz for Au_{29}^{2-} and Au_{29}^{1-}, respectively. The calculated magnetron frequencies are $\nu_- = 992$ and 1035 Hz, respectively, for the present trap parameters: magnetic field $B = 5$ T, trapping voltage $U = 12$ V, and trap dimension [23,24] $d^2 = 200\,mm^2$. The precursor and the product cluster-ion yields oscillate at opposite phase, $\phi = 76(10)°$ and $76(9)° + 180°$,[1] with a damping of $\gamma = 187(89)$ and $121(92)\,s^{-1}$, respectively. After 100 ms the oscillation has disappeared (see Fig. 4). A summary of the fit parameters is given in Table 1.

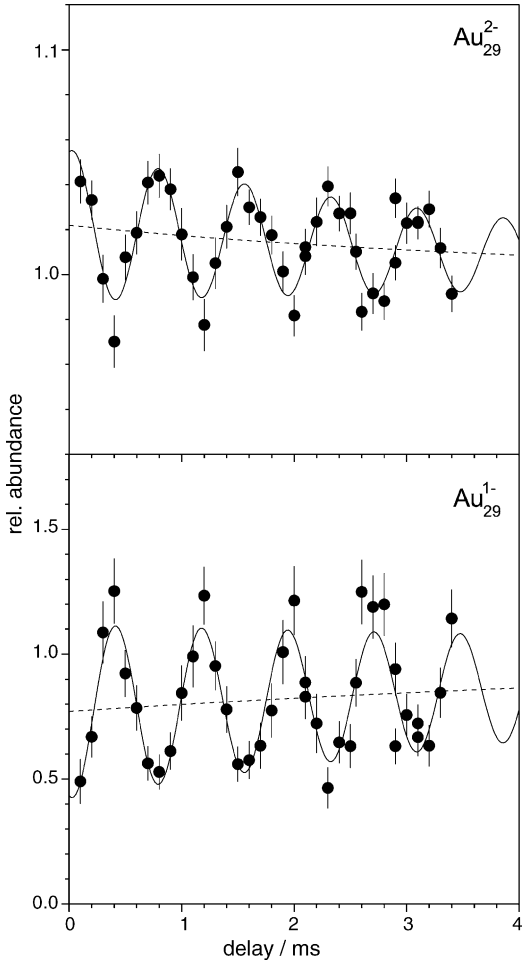

Fig. 3. Relative abundance of Au_{29}^{2-} and Au_{29}^{1-} as a function of the delay between photoexcitation and ejection for time-of-flight mass analysis. The solid line is a fit of Eq. (1) to the data points. The dashed line shows only the exponential behavior.

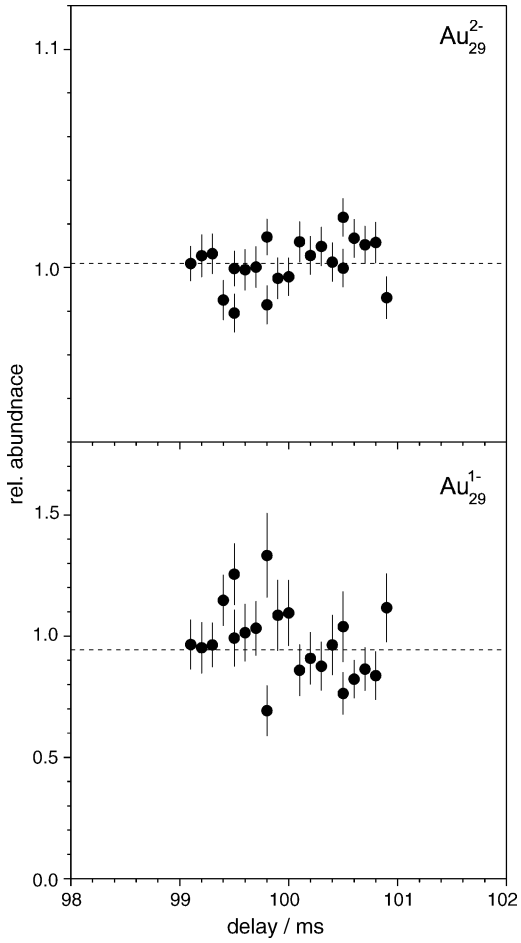

Fig. 4. Relative abundance of Au_{29}^{2-} and Au_{29}^{1-} as a function of the delay between photoexcitation and ejection for time-of-flight mass analysis. The dashed line shows the weighted mean of the data points: 1.001(2) and 0.94(3), respectively.

These findings are similar to the ones for monanions as discussed recently [22]. An increased frequency of the magnetron motion is consistent with space-charge effects. However, the origin of a coherent magnetron motion, which seems to be involved in the phenomenon, and of the opposite phases of precursors and products are not yet understood. In the following, the discussion will be restricted to the exponential behavior of precursor decay

[1] While the oscillations of the product yield is evident from the raw data, it remains an open question whether the oscillation of the precursor abundance may be an artifact of the normalization procedure.

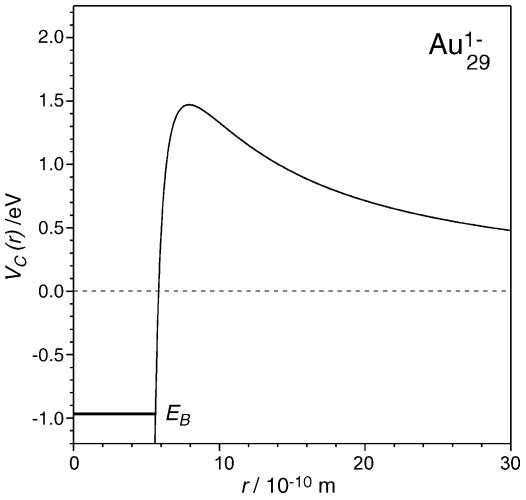

Fig. 5. Coulomb barrier of Au_{29}^{1-} as calculated from Eq. (2). The binding energy of the second surplus electron as deduced from Eq. (17), $E_B = E_A(n = 29, z = -1) = 0.97$ eV, is indicated.

and product appearance. The fit yields a life-time for Au_{29}^{2-} of $\tau = 1/k = 4.3(2.0)$ ms and an appearance time of $\tau = 7.6(5.7)$ ms for Au_{29}^{1-}. Note that even for the shortest delay times a significant number of monoanionic products are recorded as discussed at the end of the next section.

4. Discussion

The observed decay-rate is compared to the rate calculated in the framework of the Weisskopf equation, where the Coulomb barrier height is taken into account. In order to determine the barrier, the metal clusters are approximated by a conducting sphere of charge state z and radius R. With the image-charge model, where an electron approaches the sphere (with distance r from the center), the Coulomb barrier is given by [25]:

$$V_C(r, R, z) = \frac{e^2}{4\pi\varepsilon_0}\left(\frac{|z|}{r} - \frac{R^3}{2r^2(r^2 - R^2)}\right). \tag{2}$$

The Coulomb barrier height for a monanionic cluster is

$$V_{C,\max}(R, z = -1) = \frac{e^2}{8\pi\varepsilon_0 R} \tag{3}$$

and the maximum is located at a distance

$$r_{C,\max}(R, z = -1) = \frac{\sqrt{5}+1}{2}R \tag{4}$$

from the center of the metal sphere [11]. The Coulomb barrier of the present case, Au_{29}^{1-}, is plotted in Fig. 5. The height is $V_{C,\max} = 1.47$ eV at $r_{C,\max} = 7.9$ Å for a cluster radius of $R = 4.9$ Å.

The capture cross-section of an approaching electron with a kinetic energy $\varepsilon > V_0 = V_{C,\max}$ is given by [26]

$$\sigma_c(\varepsilon) = \pi R_0^2\left(1 - \frac{V_0}{\varepsilon}\right) = \sigma_{c,0}\left(1 - \frac{V_0}{\varepsilon}\right) \tag{5}$$

where $R_0 = r_{C,\max}$. In the case $\varepsilon < V_0$ the capture cross-section is $\sigma_c = 0$; the electron has not enough energy to overcome the Coulomb barrier.

The Weisskopf rate for the thermionic emission of an electron can be calculated by starting with the differential expression [27]

$$\tilde{k}(E, E_B, \varepsilon)\,d\varepsilon = \frac{2m}{\pi^2\hbar^3}\sigma_c(\varepsilon)\varepsilon\frac{\rho_M(E - E_B - \varepsilon)}{\rho_D(E)}\,d\varepsilon, \tag{6}$$

where E is the internal energy of the dianion, E_B the binding energy, and ε is the kinetic energy of the emitted electron of mass m. ρ_D and ρ_M are the level densities of the dianion and the monoanion.

Inserting the capture cross-section and integrating expression (6) yields the electron-emission rate:

$$k(E, E_B) = \frac{2m}{\pi^2\hbar^3}\sigma_{c,0}\int_{V_0}^{\infty}\varepsilon\left(1 - \frac{V_0}{\varepsilon}\right)\frac{\rho_M(E - E_B - \varepsilon)}{\rho_D(E)}\,d\varepsilon. \tag{7}$$

To calculate the integral the expression for the level density has to be inserted. From the microcanonical temperature T of a cluster with energy E the relation

$$\frac{1}{k_B T} = \frac{d}{dE}\ln\rho(E). \tag{8}$$

is known [28]. For $\varepsilon \ll E - E_B$ the level density can be approximated by [26]

$$\ln\rho(E - E_B - \varepsilon) \approx \ln\rho(E - E_B - V_0) - (\varepsilon - V_0)\frac{1}{k_B T_M}, \tag{9}$$

with the approximation applied at the maximum V_0 of the Coulomb barrier. $T_M = T(E - E_B - V_0)$ is the temperature of the product system, i.e., the monoanion. Note that the approximation in Eq. (9) does not hold for electron energies ε close to $E - E_B$. However, this tail in the energy distribution can be neglected, since in the following the exponential of the expression in Eq. (9) is used which gives no significant contribution for these higher kinetic energies ε.

Thus, the rate becomes

$$k(E, E_B) = \frac{2m}{\pi^2\hbar^3}\sigma_{c,0}\frac{\rho_M(E - E_B - V_0)}{\rho_D(E)}\exp\left(\frac{V_0}{k_B T_M}\right) \times \int_{V_0}^{\infty}\varepsilon\left(1 - \frac{V_0}{\varepsilon}\right)\exp\left(-\frac{\varepsilon}{k_B T_M}\right)d\varepsilon. \tag{10}$$

The integral is equal to

$$\int_{V_0}^{\infty}\varepsilon\left(1 - \frac{V_0}{\varepsilon}\right)\exp\left(-\frac{\varepsilon}{k_B T_M}\right)d\varepsilon = k_B^2 T_M^2\exp\left(-\frac{V_0}{k_B T_M}\right) \tag{11}$$

and the electron-emission rate reduces to

$$k(E, E_B) = \frac{2m}{\pi^2\hbar^3}\sigma_{c,0}k_B^2 T_M^2\frac{\rho_M(E - E_B - V_0)}{\rho_D(E)}. \tag{12}$$

As mentioned in [26] Eq. (8) can be rewritten as

$$\ln\rho(E) = \int_0^E \mathrm{d}E' \frac{1}{k_\mathrm{B}T(E')} = S(E), \tag{13}$$

i.e., the level densities are determined from the entropy of the clusters.

Thus, for a given energy the temperature can be calculated and the rate is given by

$$k(E, E_\mathrm{B}) = \frac{2m}{\pi^2\hbar^3}\sigma_{\mathrm{c},0}k_\mathrm{B}^2T_\mathrm{M}^2 \exp\{S(E - E_\mathrm{B} - V_0) - S(E)\}. \tag{14}$$

The temperature is determined from the energy–temperature relation

$$E(T) = n_\mathrm{eff}\int_0^T C(T')\,\mathrm{d}T'. \tag{15}$$

with the effective number of atoms $n_\mathrm{eff} = (3n-6)/3 = n-2$ [29] that takes into account the three translational and three rotational degrees of freedom of the cluster. The heat capacity values $C(T)$ are taken from bulk gold [30] where for temperatures $T > 230$ K a linear behavior is assumed with $C(T) = a_1 + 2a_2T$ and thus an energy–temperature relation

$$E(T) = n_\mathrm{eff}(a_0 + a_1T + a_2T^2), \tag{16}$$

with the fitted parameters $a_0 = -16.1$ meV, $a_1 = 0.257$ meV K^{-1}, and $a_2 = 1.51 \times 10^{-5}$ meV K^{-2} (for details see [22]). The temperature of a cluster can then be deduced by an inversion of Eq. (16).

The electron-emission rate is calculated by application of Eq. (14), where the total excitation energy is $E = E_\mathrm{ph} + E_\mathrm{th}$ with the photon energy $E_\mathrm{ph} = 2 \times 3.49$ eV (absorption of two photons), the thermal energy $E_\mathrm{th} = E(295\,\mathrm{K}) = 1.65$ eV, and the Coulomb barrier height $V_0 = 1.47$ eV for Au_{29}^{1-}. The calculated rate is matched to the experimental emission rate $k = 1/\tau$ by varying the electron binding energy E_B. The result is $E_\mathrm{B} = 0.91(5)$ eV, where only the statistical uncertainty is given.

The assumption of delayed electron emission upon the absorption of two photons is reasonable in the light of the consequences of the absorption of more or less photons. In the latter case, the clusters have not enough energy for a statistical electron loss described by the Weisskopf equation in the experimental time window. But if, on the other hand, more than two photons are absorbed, the emission happens immediately on the time scale of the present experiment. This explains the offset of the monoanion yield for very short delay times. However, this offset may also be (partly) due to a prompt direct process, where only one photon is involved and where no equilibration of the excitation energy within the cluster occurs as is assumed in the Weisskopf approach.

The measured value of the electron binding energy can be compared to the electron affinity of monoanionic gold clusters as approximated in the model of a metallic sphere. The classical expression for the electron affinity is [10]

$$E_\mathrm{A}(n, z) = W + \left(z - \frac{1}{2}\right)\frac{1}{4\pi\varepsilon_0}\frac{e^2}{R(n)}, \tag{17}$$

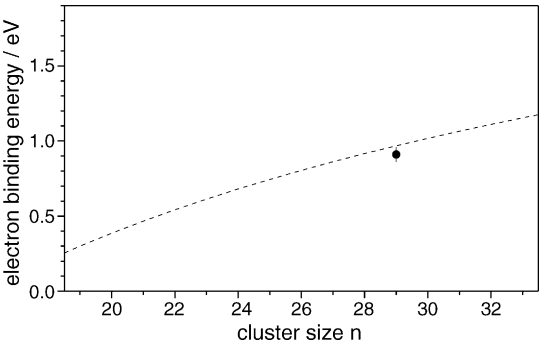

Fig. 6. Electron binding energy of Au_{29}^{2-} as compared to the second electron affinity in the LDM model (dashed line).

where a possible spill-out has been neglected. For the bulk work function $W = 5.38$ eV of gold and the radius $R(n) = r_0n^{1/3}$ (with the Wigner–Seitz-radius $r_0 = 1.59$ Å) the dashed curve of $E_\mathrm{A}(n,z=-1)$ in Fig. 6 results for the cluster monoanions. The value determined with the Weisskopf equation has been added to the figure (full circle). It agrees well with the simple model of the electron affinity.

So far only electron emission has been taken into account as a decay channel. However, for metal clusters also radiative cooling has been observed [29], where hot clusters cool by radiation of IR photons. The influence of radiative cooling on the measured electron-emission rate is not trivial. The energy loss due to IR radiation might quench the electron emission completely, i.e., the residual internal energy is not sufficient for a decay process, or the electron emission occurs at a lower rate since the internal energy is decreased. No experimental data are available for gold clusters with respect to the photon emission rate as a function of the excitation energy or temperature. However, with the assumption that the emission of a single photon lowers the internal energy below the threshold for electron detachment, the observed electron-emission rate is larger than in the absence of photon emission. Thus, the actual electron-emission rate would be smaller and consequently the electron binding energy larger than deduced above. So the value $E_\mathrm{B} = 0.91(5)$ eV can be regarded as a lower limit of the electron binding energy in the presence of radiative cooling.

5. Summary and outlook

Size and charge-state selected gold-cluster dianions Au_{29}^{2-} have been photoexcited in a Penning trap and delayed electron emission has been monitored time-resolved. In addition to the expected exponential decay an oscillation of the ion yield has been observed. As discussed elsewhere [22] the frequency could be that of the magnetron motion of the ions. However, the origin of this oscillation is unknown and further experiments are required for a thorough investigation.

The observed emission rate has been compared to the rate obtained from the Weisskopf equation, where the Coulomb barrier has been taken into account in the calculation of the capture cross-section. The rates matched for an electron binding energy $E_\mathrm{B} = 0.91(5)$ eV which is in good agreement with the second

electron affinity $E_A(n=29, z=-1) = 0.97$ eV of Au_{29} as deduced from the liquid drop model. In the presence of radiative cooling the electron binding energy $E_B = 0.91(5)$ eV resembles a lower limit.

In addition to electron emission, the evaporation of a neutral monomer may occur [13]. However, at the low fluence applied in the present investigation and for the investigated cluster size no significant corresponding product-ion yield was observed, i.e., of doubly charged Au_{28}^{2-}. Another decay channel is ion loss, i.e., the emission of both electrons from the dianion such that the cluster is neutral and leaves the ion trap [18]. A loss of 10–20% has been observed. Whether this emission process is sequential or correlated is still an open question.

Acknowledgements

This work was supported by the Deutsche Forschungsgemeinschaft (DFG) under contract no. SCH401/13-3 and the Collaborative Research Center SFB652, and the European Union within the "Cluster cooling" network under contract no. IHP-CT-2000-00026.

References

[1] Y. Shi, V.A. Spasov, K.M. Ervin, J. Chem. Phys. 111 (1999) 938.
[2] V.A. Spasov, Y. Shi, K.M. Ervin, Chem. Phys. 262 (2000) 75.
[3] A. Herlert, S. Krückeberg, L. Schweikhard, M. Vogel, C. Walther, Phys. Scr. T80 (1999) 200.
[4] C. Yannouleas, U. Landman, A. Herlert, L. Schweikhard, Phys. Rev. Lett. 86 (2001) 2996.
[5] A. Dreuw, L.S. Cederbaum, Chem. Rev. 102 (2002) 181.
[6] A. Dreuw, L.S. Cederbaum, Phys. Rev. A 63 (2001) 012501 [erratum, 049904].
[7] P. Weis, O. Hampe, S. Gilb, M.M. Kappes, Chem. Phys. Lett. 321 (2000) 426.
[8] M.N. Blom, O. Hampe, S. Gilb, P. Weis, M.M. Kappes, J. Chem. Phys. 115 (2001) 3690.
[9] O. Hampe, M. Neumaier, M.N. Blom, M.M. Kappes, Chem. Phys. Lett. 354 (2002) 303.
[10] A. Herlert, L. Schweikhard, Int. J. Mass Spectrom. 229 (2003) 19.
[11] L. Schweikhard, A. Herlert, S. Krückeberg, M. Vogel, C. Walther, Philos. Mag. B 79 (1999) 1343.
[12] A. Herlert, L. Schweikhard, M. Vogel, Eur. Phys. J. D 16 (2001) 65.
[13] L. Schweikhard, K. Hansen, A. Herlert, M.D. Herráiz Lablanca, G. Marx, M. Vogel, Hyperfine Interact. 146/147 (2003) 275.
[14] A. Herlert, L. Schweikhard, Int. J. Mass Spectrom. 234 (2004) 161.
[15] U. Hild, G. Dietrich, S. Krückeberg, M. Lindinger, K. Lützenkirchen, L. Schweikhard, C. Walther, J. Ziegler, Phys. Rev. A 57 (1998) 2786.
[16] M. Vogel, K. Hansen, A. Herlert, L. Schweikhard, Phys. Rev. Lett. 87 (2001) 013401.
[17] M. Vogel, K. Hansen, A. Herlert, L. Schweikhard, J. Phys. B: At. Mol. Opt. Phys. 36 (2003) 1073.
[18] L. Schweikhard, K. Hansen, A. Herlert, G. Marx, M. Vogel, Eur. Phys. J. D 24 (2003) 137.
[19] G. Savard, St. Becker, G. Bollen, H.-J. Kluge, R.B. Moore, Th. Otto, L. Schweikhard, H. Stolzenberg, U. Wiess, Phys. Lett. A 158 (1991) 247.
[20] D.A. Laude, S.C. Beu, Anal. Chem. 61 (1989) 2422.
[21] C. Walther, St. Becker, G. Dietrich, H.-J. Kluge, M. Lindinger, K. Lützenkirchen, L. Schweikhard, J. Ziegler, Z. Phys. D 38 (1996) 51.
[22] A. Herlert, L. Schweikhard, Int. J. Mass Spectrom. 249–250 (2006) 215.
[23] L.S. Brown, G. Gabrielse, Rev. Mod. Phys. 58 (1986) 233.
[24] L. Schweikhard, J. Ziegler, H. Bopp, K. Lützenkirchen, Int. J. Mass Spectrom. Ion Process. 141 (1995) 77.
[25] J.D. Jackson, Classical Electrodynamics, second ed., John Wiley & Sons, New York, 1975.
[26] V. Weisskopf, Phys. Rev. 52 (1937) 295.
[27] J.U. Andersen, E. Bonderup, K. Hansen, J. Phys. B: At. Mol. Opt. Phys. 35 (2002) R1.
[28] K. Hansen, U. Näher, Phys. Rev. A 60 (1999) 1240.
[29] C. Walther, G. Dietrich, W. Dostal, K. Hansen, S. Krückeberg, K. Lützenkirchen, L. Schweikhard, Phys. Rev. Lett. 83 (1999) 3816.
[30] Gmelins Handbuch der Anorganischen Chemie, vol. 8, Auflage, Gmelin-Institut für Anorganische Chemie (Hrsg.), Verlag Chemie GmbH, Weinheim/Bergstrasse, 1954.